Investigation of Phase Formation Sequence in the Iron–Aluminum Phase Diagram Using Superlattice Composites as Reactants

Christopher A. Grant and David C. Johnson*

Department of Chemistry and Materials Science Institute, University of Oregon, Eugene, Oregon 97403

The low-temperature reaction of iron–aluminum superlattice composites as a function of composition and layer thicknesses was explored. Samples were largely amorphous but with embedded nanocrystalline FeAl or α-Fe in the as-deposited state. It was not generally possible to form a homogeneous amorphous alloy via a solid-state amorphization reaction. In most of the composites investigated, FeAl was the first interfacial compound observed to form regardless of layer thicknesses or overall composition. The second phase formed was Fe_2Al_5. Several exceptions to this general behavior were seen, however, illustrating the kinetic nature of the nucleation process. It is suggested that FeAl generally formed first for two reasons. The first is the extremely wide combined stability field of disordered bcc α-Fe and ordered bcc FeAl. Because the starting multilayer had a large number of interfaces, and because intermixing at these interfaces appears to have been relatively high, a significant fraction of the starting multilayer must have had a composition falling within this broad stability field, making it easy for crystallites of the bcc material to form. The second reason is that FeAl has a small unit cell, containing only two atoms. All other binary Fe/Al phases have larger unit cells.

Introduction

A key characteristic of molecular synthesis is the use of kinetic control to direct the reaction path. In solid-state syntheses, slow diffusion rates dictate high temperatures and long reaction times.[1] Under such conditions, solid-state reactions generally yield a mixture of the thermodynamically most stable phases.[2] In general, it is not possible to apply kinetic control to a solid-state synthesis, and one is more or less at the mercy of the phase diagram with respect to which product phases are formed.

In the early 1980's, Schwarz and Johnson[3] found that kinetically stable amorphous metal alloys could be formed by low-temperature, solid-state reaction of alternating thin layers of crystalline elements. This interdiffusion reaction was found to be driven by the large negative heat of mixing between the constituents such that the amorphous alloy has a lower free energy than the initial layered structure and the growth of the amorphous layer between the reacting layers was found to be diffusion-controlled. Since the growth rate decreases with increasing thickness of the amorphous layer, nucleation of the thermodynamically more stable crystalline compound eventually occurs on a time-scale comparable to further growth of the amorphous phase. Therefore, there exists a critical layer thickness for the elemental layers within a composite which reflects the energetics of both the diffusion and nucleation processes. If the composites contain layers with thickness below this critical value, the system will evolve into a bulk amorphous solid.[4] Early work on nickel–zirconium thin

film diffusion couples showed that the critical layer thickness can be on the order of hundreds of angstroms.[5] Similarly large critical layer thicknesses have been found in approximately 30 other metal–metal and metal-metalloid systems. The term solid-state amorphization reaction has been used to describe this reaction.[6]

Recently, Novet and Johnson reported a synthetic technique which allows the direct synthesis of individual solid phases using a solid-state amorphization reaction to prepare an amorphous intermediate.[7] In this method, a multilayer stack of thin amorphous elemental layers is prepared under vacuum. The layer thicknesses are chosen to be less than the critical thickness so that the entire multilayer can be diffused into a homogeneous, amorphous state using only gentle heat. At this point, nucleation rather than diffusion becomes the limiting factor in the reaction. The material, it was argued, that will nucleate most easily from a homogeneous, amorphous intermediate is the stoichiometric phase closest in composition to the amorphous material. If this is so, then it should be possible to produce any desired phase directly simply by adjusting the stoichiometry of the initial multilayer. The authors showed that this technique works as desired in the system consisting of iron and silicon.

The generality of this synthetic approach depends on the ability to prepare an amorphous alloy as a reaction intermediate. In general, the phase diagrams in which solid-state amorphization reactions have been found are dominated by line phases. Few systems with large regions of solid solubility and relatively few metal–nonmetal systems have been explored. Also, metal–metal systems studied to date have only been explored down to layer

---

* To whom correspondence should be addressed.
● Abstract published in *Advance ACS Abstracts*, June 15, 1994.
(1) Brewer, L. *J. Chem. Educ.* **1958**, *35*, 153.
(2) Brophy, J. H.; Rose, R. M.; Wulff, J. *The Structure and Properties of Materials*; John Wiley and Sons: New York, 1964; Vol. 2, pp 91–94.
(3) Schwarz, R. B.; Johnson, W. L. *Phys. Rev. Lett.* **1983**, *51*, 415–418.
(4) Gösele, U.; Tu, K. N. *J. Appl. Phys.* **1989**, *66*, 2619–2626.

(5) Cotts, E. J.; Meng, W. J.; Johnson, W. L. *Phys. Rev. Lett.* **1986**, *57*, 2295–2298.
(6) Clemens, B. M.; Sinclair, R. *MRS Bull.* **1990**, *15*, 19–28.
(7) Novet, T.; Johnson, D. C. *J. Am. Chem. Soc.* **1991**, *113*, 3398–3403.

thicknesses of approximately 30 Å. This paper reports the results of our investigation of the initial reactions occurring in the binary iron–aluminum system as a function of layer thickness (down to layer thicknesses of 4 Å) and composition of the initial layered composite. The iron–aluminum system was chosen as it differs from most phase diagrams in which solid-state amorphization reactions have been observed by containing a compound, FeAl, with an exceedingly broad region of nonstoichiometry. We compare our results with earlier investigations of the evolution of iron–aluminum thin film diffusion couples and co-deposited materials.

Experimental Methods

Preparation of Samples. Samples were prepared by sequential e-beam evaporation of Fe 99.99% (Aesar REaction 12958) and Al 99.999% (Aesar 10573A) in a computer-controlled vacuum chamber, the design and operation of which are described elsewhere.[8] Deposition took place at pressures of $<2 \times 10^{-7}$ Torr, and deposition rates for both Fe and Al were adjusted to 0.5 Å/s. Polished, oxidized 4-in silicon wafers coated with a layer of poly-(methyl methacrylate) (PMMA) were used as substrates. The size of the wafer insured that multiple analyses could be performed on each sample. The PMMA coating was applied using a spin coater and a 3% solution of high molecular weight PMMA in chlorobenzene. When a sample deposited on such a PMMA-coated substrate is immersed in acetone, the PMMA dissolves and the multilayer floats free of the silicon substrate. It was found convenient to use multilayers removed from their substrates in this manner for a number of analytical techniques. The substrate temperature during deposition was neither monitored nor controlled.

Determination of Stoichiometry. Driven quartz crystal rate monitors were used to control deposition of the individual layers in each multilayer sample. Accumulation of an elemental layer was allowed to proceed until the rate monitor reported that the desired layer thickness had been achieved, at which time a shutter was closed over the e-beam gun and the substrate was repositioned in preparation for deposition of the next elemental layer. However, the layer thickness reported was simply the time-integrated rate measured by the rate monitor. The monitors determine rate based on density and Z ratio values which are unique for each element and must be entered by the operator. Because they were so thin, the individual layers in samples prepared for this study were noncrystalline, and therefore their density was unknown. Although it would have been possible to calculate a scaling factor that related intended thickness to actual thickness, lack of information about sample density meant that it was not possible to use thickness alone to determine sample stoichiometry. Instead, neutron activation analysis (NAA) was performed on a series of multilayer samples to find Fe:Al ratios. A calibration curve was constructed which allowed determination of thickness values which should be entered in the rate monitors in order to obtain a given stoichiometry. Subsequent samples were prepared using this calibration curve.

Differential Scanning Calorimetry (DSC). The thermal evolution of the samples as they were subjected to elevated temperatures was monitored using DSC. A TA Instruments TA9000 calorimeter fitted with a 910DSC cell was used. Approximately 0.5 mg of sample was removed from the substrate as described above and collected into an aluminum DSC pan. This was dried under vacuum to remove residual acetone and then crimped shut. An empty pan was used as the reference. The sample was heated from ambient temperature to 550 °C at 10 °C/min under flowing nitrogen and then allowed to cool to room temperature. Without disturbing the sample or instrument in any way, this cycle was repeated two more times. The net heat flow associated with irreversible changes in the sample was found by subtracting the data for the third heating from the first. A measure of the repeatability of the experiment and of the degree

Table 1. Layer Thickness Data for Samples Prepared

sample stoichiometry	requested layer thickness (Å)		d spacing (Å)	estimated layer thickness (Å)	
	Fe	Al		Fe	Al
$Fe_{1.0}Al_{1.0}$	8	9	19	8	11
$Fe_{1.0}Al_{2.0}$	8	18	29 ± 2	8 ± 1	21 ± 1
$Fe_{2.0}Al_{5.0}$	8	23	38	8	29

to which any irreversible changes had gone to completion during the first heating was found by subtracting the data for the third heating from the second.

X-ray Diffraction (XRD). Diffraction data were collected using a Scintag XDS 2000 θ–θ diffractometer. A custom-built sample stage, designed to allow precise alignment of sample height and angle, was used. To confirm layering within the sample, grazing-angle XRD was performed. To identify crystalline phases present, high-angle XRD was performed on samples that had been removed from the silicon substrates and collected onto glass slides.

Transmission Electron Microscopy (TEM). Transmission electron microscopy was performed using a Phillips CM12 analytical electron microscope operated at 100 keV. After deposition, samples were lifted from the substrate and dried onto TEM support grids, allowing plan-view imaging of the multilayer sample. The samples were studied, looking for crystallites which might act as nucleation sites in the film.

Results

A number of multilayer samples with compositions corresponding to the stoichiometries FeAl, FeAl₂, and Fe₂-Al₅ were prepared. The requested elemental layer thickness values used were based on the NAA derived calibration data and were chosen to give the desired stoichiometries. The precise values of the actual layer thicknesses were not determined, but their values can be approximated by looking at the d spacing (size of the repeat unit in the multilayer stack) for each sample as found by grazing-angle XRD. These data are summarized in Table 1. In the table, d spacing represents the position of the first-order Bragg peak, uncorrected for index of refraction effects. Estimated layer thickness assumes perfect stoichiometry. Uncertainty for samples of stoichiometry $Fe_{1.0}Al_{2.0}$ was determined based on a sample size of $N = 11$. Insufficient data were available to determine statistics for the other two stoichiometries, but they are expected to be of the same magnitude.

Each sample was divided into several pieces and analyzed as follows. A grazing-angle XRD trace was taken. If the sample showed no layering, or a d spacing dramatically different from that expected, the sample was discarded. A DSC trace was taken. This indicated at what temperatures changes in the sample took place but did not tell what those changes were. For each temperature of interest, a new portion of the sample was heated once to the desired temperature, allowed to cool, and collected onto a glass slide. High-angle XRD data were then collected. The heating was done under flowing nitrogen using the DSC cell and a ramp rate of 10 °C/min. By looking at the phases present in the sample at a temperature just below a transformation as indicated by DSC, and at a temperature above the transformation, it was possible to determine the nature of the transformation.

Grazing-Angle X-ray Diffraction. In general, the grazing angle XRD spectra of the samples prepared in this study contained Bragg diffraction peaks out to a d spacing of 10–15 Å. Subsidiary maxima, resulting from the incomplete destructive interference of the reflections from each of the layers as well as front surface to back

(8) Fister, L.; Li, X.-M.; McConnell, J.; Novet, T.; Johnson, D. C. *J. Vac. Sci. Technol.* **1993**, *11*, 3014–3019.
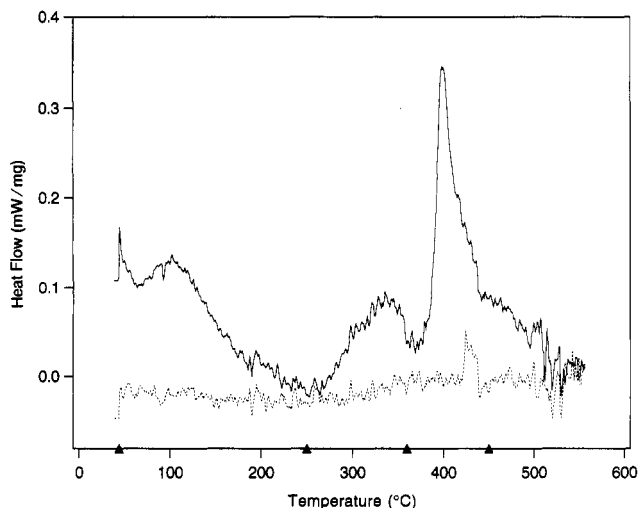
Figure 1. Differential scanning calorimetry data obtained for the reaction of a superlattice having a repeat unit of 8-Å iron and 18-Å aluminum. The upper curve was obtained by heating the sample at 10 °C/min and subtracting a second run on the same sample obtained under identical conditions. The lower curve is the difference between the heat flow rates of the second and third heating of the same sample and give a measure of the repeatability of the experiment.

surface interference were observed out to the same angular range. The intensity of the Bragg diffraction peaks decayed quickly toward higher diffraction angles. This implies that the samples did not contain abrupt interfaces but rather the iron and aluminum were interdiffused on a length scale approaching 15 Å. The ability to observe subsidiary maxima out to 6–7° implies that the layer-to-layer spacing of that region of the sample contributing to the diffraction pattern was very regular, with variations of less than 1 Å between high and low spots within the diffracting regions. To confirm the smoothness of the layering, STM experiments were performed on several samples. The surfaces of the samples were significantly contoured with height variations approaching 100 Å. This suggests that only small portions of the samples contribute to the observed diffraction patterns. The STM results are consistent with the high X-ray flux required to observe the second Bragg diffraction peaks from the multilayers.

Fe$_{1.0}$Al$_{2.0}$. A total of nine samples with intended thicknesses 8-Å Fe and 18-Å Al were analyzed by DSC. All showed two exothermic peaks, one of which fell between 400 and 450 °C, and the other which generally fell between 225 and 350 °C. DSC data for one such sample are shown in Figure 1. XRD patterns were taken after the sample had been heated to various temperatures. Figure 2 shows such XRD patterns, collected from the same sample after it had been heated to the temperatures indicated by markers on the temperature axis in Figure 1. In the as-deposited condition, the sample produced a broad (3.5° fwhm) diffraction feature centered at 43.5° which is consistent with small crystallites of either FeAl or Fe. TEM data confirmed the presence of very small grains of crystalline material. At 250 °C, just before the first exotherm, the intensity of the diffraction maximum had increased in intensity and narrowed, indicating that there were more crystallites with larger average size. At 360 °C, between the first and second exotherms, FeAl was seen to be present. At 450 °C, after the second exotherm, the XRD pattern showed peaks characteristic of both FeAl and Fe$_2$Al$_5$. The XRD pattern for the sample after it had
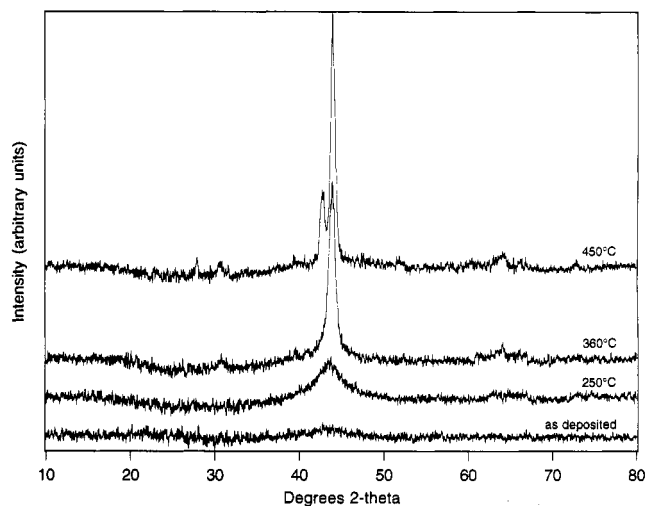

Figure 2. X-ray diffraction data collected during reaction of the superlattice described in Figure 1. The indicated temperatures correspond to the markers on the bottom axis of Figure 1.
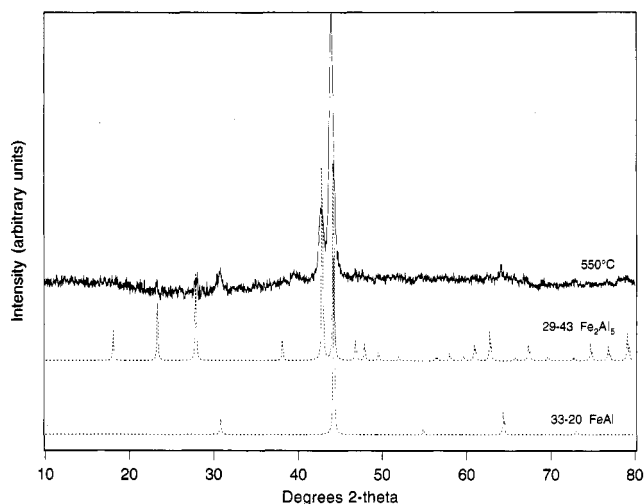

Figure 3. X-ray diffraction pattern for the superlattice described in Figures 1 and 2 after it had been heated to 550 °C. Superimposed on this pattern are the XRD patterns synthesized from the JCPDS cards for FeAl (33–20) and Fe$_2$Al$_5$ (29–43), demonstrating that both of these compounds were present in the sample.

been heated to 550 °C is shown in Figure 3. Superimposed on this pattern are the XRD patterns synthesized from the JCPDS cards for FeAl and Fe$_2$Al$_5$, demonstrating that both these compounds were present in the sample. No FeAl$_2$ was detected in any of the samples. These data demonstrate that FeAl is the first phase to form at the interface between iron and aluminum and that Fe$_2$Al$_5$ is the second phase which forms.

In addition, four samples with intended thicknesses 4-Å Fe and 9-Å Al were examined. Results for these were ambiguous. All samples appeared by XRD to be amorphous as-deposited, although the presence of small crystallites of either Fe or FeAl cannot be ruled out by the diffraction data alone. DSC data for two of the samples showed a single strong exotherm near 300 °C. This was found to correspond with the appearance of FeAl in the XRD data. No other phases were detectable by XRD, even after the samples were heated to 550 °C. The third sample showed a strong exotherm near 350 °C, and the DSC of the final sample did not show anything clearly recognizable as an exotherm. After being heated to 550

°C, XRD of these latter two samples showed FeAl strongly and a weak signal that might be caused by Fe_2Al_5.

$Fe_{2.0}Al_{5.0}$. A total of five samples with intended thicknesses 8-Å Fe and 23-Å Al were analyzed by DSC. Most showed two exotherms, one of which fell at or just above 400 °C, and the other which fell below 300 °C. Once again, the lower temperature exotherm was found to coincide with the appearance of FeAl, while above the second exotherm, both FeAl and Fe_2Al_5 were found to be present. All of these samples showed both phases present at 550 °C. In two of the samples, the lower temperature exotherm was missing and the exotherm at 400 °C was very sharp and appeared to consist of two superimposed peaks. XRD data indicated that FeAl did not form in one of these samples, where only Fe_2Al_5 was present after heating past the high-temperature exotherm (550 °C). All samples were amorphous by XRD in the as-deposited state.

$Fe_{1.0}Al_{1.0}$. A total of four samples with intended thicknesses 8-Å Fe and 9-Å Al were analyzed by DSC. All showed a weak exotherm below 200 °C and a strong exotherm at 400 °C. The samples showed a single broad crystalline peak in the as-deposited state that may be FeAl. Samples heated to 310 °C showed FeAl present. Samples heated to 550 °C showed FeAl and an unidentified phase with weak X-ray diffraction maxima. No Fe_2Al_5 was detectable. One of the samples showed an additional strong exotherm at 330 °C. The XRD signal arising from the unidentified phase was weak in all samples except this one, in which the signal was as strong as that for FeAl. Further attempts to isolate this unknown phase are planned.

Discussion and Conclusions

It has for some time been understood that when a bulk diffusion couple, one which involves macroscopic amounts of material, is heated, a mixture of phases results.[9] In fact, every phase stable at the annealing temperature will eventually appear. For this reason, bulk diffusion couples have been used with success to probe phase diagrams.[2]

Thin-film diffusion couples, in which the starting layers are crystalline and vary in thickness from a few hundred to several thousand angstroms, have been studied since the 1970s.[10-12] In these, it was found that a single phase nucleates at the interface between starting materials and grows until one of the starting materials has been exhausted. Only then does a second phase nucleate and begin to grow. Thus, phases appear one at a time, sequentially. It was found, however, that no matter the relative thicknesses of the starting layers, for a given binary system, the same phase always appeared first. So consistent was this phenomenon, that empirical rules were formulated for metal–silicon[13] and metal–metal[14,15] systems which correctly predicted the first phase to nucleate in the large majority of systems.

Novet and Johnson[7] reported a synthetic technique whose intent was to give the chemist control over which phase appears in solid-state reaction. The goal was to convert the starting materials to a homogeneous, amorphous intermediate quickly and gently enough that no (undesired) crystalline phases would have time to form. It was hoped that the phase that would crystallize from this intermediate would be the one whose stoichiometry was closest in composition to that of the amorphous intermediate, thus allowing the product to be determined simply by varying the composition of the starting multilayer. Using iron and silicon, they were in fact able to nucleate directly every phase in the Fe/Si phase diagram, thereby bypassing the first-phase rule.

The Fe/Al phase diagram includes two stable ordered phases (Fe_3Al, FeAl) and three stable intermetallic phases ($FeAl_2$, Fe_2Al_5, $FeAl_3$).[16,17] We also note that the solubility of Al in Fe is quite high (up to 45%). Samples prepared for this study fall toward the center of the composition range (50–71 at. % Al), covering FeAl, $FeAl_2$, and Fe_2Al_5. We had hoped to form each of these phases directly from the starting materials in a manner analogous to the work involving iron and silicon by forming an amorphous alloy as a reaction intermediate. Instead, we discovered behavior more typical of thin-film diffusion couples. In every case, FeAl was found to appear first, followed by Fe_2Al_5. In no case was $FeAl_2$ detected. Neither of the cited first-phase rules predict FeAl as the first phase, nor is this situation consistent with previous work involving Fe/Al thin films.

Although it should be possible in principle to produce an amorphous Fe/Al alloy in the composition range studied,[18] it appears difficult to do so. Chen et al.[19] report success in obtaining amorphous Fe/Al alloys but only by using cosputtering and substrates cooled to liquid nitrogen temperatures. On the other hand, Sumiyama et al.[20] were able to form an amorphous alloy only in the range 0.65–0.95 at. % Al, even using liquid nitrogen cooled substrates. At lower Al concentrations, the disordered bcc material was formed. In this study, most of the starting multilayers investigated appear to be amorphous when examined by XRD. TEM data, however, reveal nanocrystalline particles dispersed throughout the amorphous base material. This situation has been described before by Wang et al.,[21] who concluded that their crystalline particles were Fe. As noted already, Al dissolves readily in α-Fe across a wide composition range to form a disordered bcc phase.[16] The compound, FeAl, has an ordered bcc structure,[17] also exists across a wide composition range, and can accommodate many vacancies.[22] The wide composition range and simple unit cell of these structures should make them easy to form. The similarity of structure between the two bcc phases suggest that if nanocrystalline α-Fe was present in the as-deposited multilayers, these particles could easily have acted as seeds for the growth of FeAl. It is also possible that some or all of the particles in the starting layers were FeAl which simply grew when the samples were annealed. Whether it was one or the other, the

(9) Lustman, M.; Mehl, R. F. *AIME Trans.* **1942**, *147*, 365–395.

(10) Ottaviani, G. *J. Vac. Sci. Technol.* **1979**, *16*, 1112–1119.

(11) Tsaur, B. Y.; Lau, S. S.; Mayer, J. W.; Nicolet, M.-A. *Appl. Phys. Lett.* **1981**, *38*, 922–924.

(12) Colgan, E. G.; Nastasi, M.; Mayer, J. W. *J. Appl. Phys.* **1985**, *58*, 4125–4129.

(13) Walser, R. M.; Bené, R. W. *Appl. Phys. Lett.* **1976**, *28*, 624–625.

(14) Bené, R. W. *Appl. Phys. Lett.* **1982**, *41*, 529–531.

(15) Colgan, E. G.; Mayer, J. W. *J. Mater. Res.* **1989**, *4*, 815–820.

(16) In *Binary Alloy Phase Diagrams*, 2nd ed.; Massalski, T. B., Bennet, L. H., Murray, J. L., Baker, H., Eds.; ASM International: Metals Park, OH, 1990; Vol. 1, pp 147–149.

(17) Villars, P.; Calvert, L. D. *Pearson's Handbook of Crystallographic Data for Intermetallic Phases*, 2nd ed.; ASM International: Materials Park, OH, 1991; Vol. 1, pp 815–817.

(18) He, Y.; Poon, S. J.; Shiflet, G. J. *Science* **1988**, *241*, 1639–1642.

(19) Chen, Q.-M.; Fan, Y.-D.; Li, H.-D. *Mater. Lett.* **1988**, *6*, 311–315.

(20) Sumiyama, K.; Hirose, Y.; Nakamura, Y. *J. Phys. Soc. Jpn.* **1990**, *59*, 2963–2970.

(21) Wang, W. H.; Xiao, K. Q.; Dong, Y. D.; He, Y. Z. *J. Non-Cryst. Solids* **1990**, *124*, 82–85.

(22) Paris, D.; Lesbats, P. *J. Nucl. Mater.* **1978**, *69 & 70*, 628–632.

presence of nanocrystalline bcc material in the starting multilayers probably prevented the samples from reaching a homogeneous, amorphous state.

The appearance of FeAl as the first crystalline phase from a solid-state reaction between pure elemental Fe and Al runs counter to both of the published first-phase rules relevant to this system and is inconsistent with results found by others investigating thin-film Fe/Al systems. The first-phase rule of Bené for metal–metal systems[14] predicts $FeAl_3$ to be the first crystalline phase to appear. That of Colgan and Mayer,[15] applicable only to aluminides, predicts that the most aluminum-rich phase will nucleate first but that this phase may be skipped if it has a large unit cell or unusually complex crystal structure.[23] Therefore, it either predicts that $FeAl_3$, or the metastable phase $FeAl_6$ will appear first, depending on whether one interprets the rule to include metastable phases. Two studies involving Fe/Al thin films have been published. In the first study,[24,25] the first phase to appear was Fe_2Al_5 at 327 °C. If one considers that the unit cell of Fe_2Al_5 contains 16 atoms ($oC16$),[17] whereas that of $FeAl_3$ contains 102 atoms ($mC102$),[17] this result could be argued to be consistent with the first-phase rule of Colgan and Mayer. The second study[26] found that $FeAl_6$ at 250 °C was the first phase to form. Once again, this result is arguably consistent with the first-phase rule. In both of these studies, the starting layers were crystalline.

In the present study, FeAl is almost always the first phase to appear. Evidently, the combination of ultrathin layering and the mostly amorphous state of the starting layers engenders behavior distinctly different from that described in the two thin-film studies. It is suggested that FeAl forms first for two reasons. The first is the extremely wide combined stability field of disordered bcc α-Fe and ordered bcc FeAl. Because the starting multilayer has a large number of interfaces and because intermixing at these interfaces appears to be relatively high, a significant fraction of the starting multilayer must have a composition which falls within this broad stability field, making it easy for crystallites of the bcc material to form. This hypothesis is supported by the fact that thinner layering more readily yields FeAl, even for the samples of composition $Fe_{1.0}Al_{2.0}$ where two sets of samples with different d spacings were examined. The thinner the

layers, the greater the fraction of the sample which can be considered interfacial region. The second reason is that FeAl has a small unit cell, containing only two atoms ($cP2$).[17,27] All other binary Fe/Al phases have larger unit cells. The next smallest unit cell belongs to Fe_2Al_5, which includes 16 atoms in its unit cell. It has been noted in the past that their large unit cell and complex structure retard formation of stoichiometric compounds in the Fe/Al system.[28] It therefore seems reasonable to suppose that a sample whose overall composition corresponds to one of the stoichiometric phases will nucleate FeAl first if portions of the sample fall within the stability field for FeAl.

In summary, a series of ultrathin multilayer samples having compositions $Fe_{1.0}Al_{1.0}$, $Fe_{1.0}Al_{2.0}$, and $Fe_{2.0}Al_{5.0}$ were prepared. In nearly every case, FeAl formed below 350 °C and was the first crystalline phase to appear upon annealing. Generally, Fe_2Al_5 appeared as a second phase near 400 °C. Samples were largely amorphous but with embedded nanocrystalline particles in the as-deposited state. This prevented formation of a homogeneous amorphous intermediate. When ultrathin multilayers are used as reactants in a solid-state synthesis, it is not sufficient that the starting elemental layers simply be ultrathin in order to form a homogeneous, amorphous intermediate. Consideration must also be given to the relative complexities of the crystal structures of phases in the system being investigated. In a system which includes several complex phases and one simple, easily formed phase, the latter may form preferentially. That is, in some cases, complexity of crystal structure may be more important than the composition of the starting multilayer in determining which crystalline phase forms.

(23) Colgan, E. G. *Mater. Sci. Rep.* **1990**, *5*, 1–44.

(24) Teixeira, S. R.; Dionisio, P. H.; da Silveira, E. F.; Freire, F. L., Jr.; Schreiner, W. H.; Baumvol, I. J. R. *Mater. Sci. Eng.* **1987**, *96*, 267–277.

(25) Teixeira, S. R.; dos Santos, C. A.; Dionisio, P. H.; Schreiner, W. H.; Baumvol, I. J. R. *Mater. Sci. Eng.* **1987**, *96*, 285–293.

(26) Csanády, A.; Günter, J. R.; Barna, P. B.; Mayer, J. *Thin Solid Films* **1988**, *167*, 203–215.

(27) We note that *Binary Alloy Phase Diagrams*, cited herein as ref 16, assigns a Pearson symbol of *cP8* to FeAl. We believe that this is a typographical error, which should read *cP2*, for the following reasons: the same reference assigns *cP2* to similar structures (CsCl, NiAl); *Pearson's Handbook of Crystallographic Data for Intermetallic Phases*, cited herein as ref 17, assigns a Pearson symbol of *cP2* to FeAl; a unit cell for FeAl which is both *cP8* and bcc does not seem credible.

(28) Masui, K.; Maruno, S.; Sakakibara, S.; Kawaguchi, T. *J. Non-Cryst. Solids* **1985**, *74*, 271–284.